

# Enhanced Properties of UV Curable Films Containing Layered Silicates as the Nanomaterial

Fawn M. Uhl<sup>a</sup>, Brian R. Hinderliter<sup>b</sup>, Prashanth Davuluri<sup>c</sup>, Stuart G. Croll<sup>b</sup>,  
Shing Chung Wong<sup>c</sup>, and Dean C. Webster<sup>b</sup>

<sup>a</sup>Center for Nanoscale Science and Engineering

<sup>b</sup>Department of Polymers and Coatings

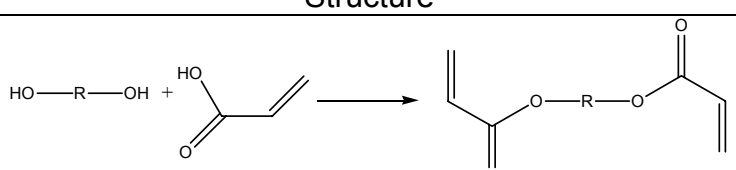
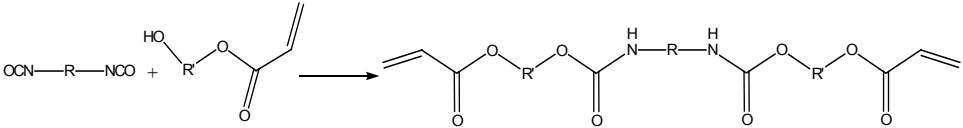
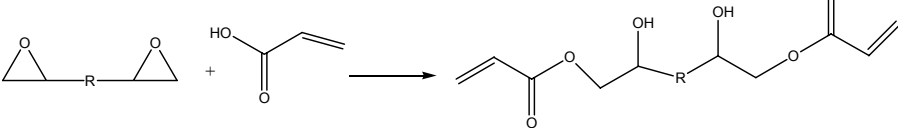
<sup>c</sup>Department of Mechanical Engineering and Applied Mechanics  
North Dakota State University, P.O. Box 5376, Fargo, ND 58105

## Introduction

UV curable films possess desirable properties such as rapid cure, solvent free characteristics, application versatility, low energy requirements, and low temperature operation making them attractive for use in the micro- and consumer electronics industries.<sup>1, 2</sup> Depending on the processing conditions and end use requirements, it is desirable to formulate polymer film systems with higher glass transition temperatures, good barrier properties, low shrinkage, flexibility, and enhanced mechanical properties.

Acrylate compounds are the main systems used in the free radical radiation cure industry.<sup>3</sup> Acrylate oligomers can be of low to high molecular weight and low to high viscosity. The oligomeric acrylates can have a urethane (aliphatic or aromatic), polyester, polyether, or epoxy structure. **Table 1** illustrates some chemistries used to form acrylated compounds.<sup>4</sup>

**Table 1.** Some chemistries to form the various acrylate systems.

Acrylate name	Structure
Polyester/ether acrylates	
Urethane acrylates	
Epoxide acrylates	

Final properties of the acrylate systems are dependent upon the chemical structure of the functionalized oligomer and monomer utilized. It has been shown by Schwalm et al. that the properties of the final product are determined by the type of acrylate system.<sup>5</sup> The use of an aliphatic oligomer leads to a final product with a low modulus while an aromatic structure leads to a final product that is hard and glassy. They have shown that the hardness and flexibility of

acrylate systems is dependent upon the type of structure utilized, **Table 2**.<sup>6</sup> Viscosity is an issue for a variety of acrylate systems therefore a reactive diluent is typically used to generate a system with the desired viscosity. Acrylate systems have been shown to have high crosslink densities and are chemical, heat, and radiation resistant.

**Table 2.** Properties of various acrylate systems.

Structure	Properties
Aromatic epoxy acrylate	Hard and brittle*
Aliphatic epoxy acrylate	Flexible, less hardness than aromatics*
Polyester acrylates	Hard to flexible, tough, solvent resistance, poor adhesion, poor alkali resistance
Urethane acrylates	Range from most flexible and soft to hard and less flexible, abrasion and impact resistance

\*Good adhesion, chemical resistance, and thermal stability

Clay-polymer nanocomposites have been prepared by in situ polymerization or melt blending. The preparation of nanoclay reinforced polymers has been shown to lead to one of several morphologies; conventional, intercalated or exfoliated composites.<sup>7, 8</sup> A conventional composite is one in which the clay aggregates are dispersed as separated phases in the polymer matrix. Intercalated composites occur when there is insertion of polymer between the clay layers. Exfoliated nanocomposites are formed when the clay layers are randomly dispersed within the polymer matrix and optical transparency is not lost. Exfoliated morphology is often cited as the desired form of morphology for optimal barrier and mechanical performance in clay-type nanocomposites. It has been shown that an enhancement in polymer properties is observed, such as improved mechanical and barrier properties, thermal stability, and chemical resistance at low loadings of clay.<sup>7-12</sup> These properties make nanoclay reinforced polymers attractive in a number applications. This paper will examine several properties of UV curable clay-acrylate formulations in which the acrylate oligomers studied are an aliphatic urethane acrylate, bisphenol A epoxy acrylate, and a polyester acrylate.

## Experimental

**Materials.** Nanomer I.31PS onium ion modified montmorillonite was supplied by Nanocor Inc. CN929, a trifunctional urethane acrylate oligomer; CN121, a difunctional bisphenol A epoxy acrylate oligomer; CN2251, a trifunctional polyester acrylate oligomer; CN2274, a polyester acrylate oligomer; and SR454, an ethoxylated (3) trimethylolpropane triacrylate, were obtained from Sartomer. The photoinitiator Darocur 1173, 2-hydroxy-2-methyl-1-phenylpropane-1-one, was obtained from Ciba Specialty Chemicals.

**Characterization** UV curing of samples was performed using a Dymax light source with a 200 EC silver lamp (UV-A, 365 nm). The intensity was 35 mW/cm<sup>2</sup> measured using a NIST Traceable Radiometer, International Light model IL1400A. Curing of panels was performed in air. Samples were drawn down onto an aluminum panel using a #1 Gardco casting bar with a gap of 4 mil. X-ray powder diffraction (XRD) data were collected using a Phillips PW3040 X'pert-MPD Multipurpose Diffractometer in Bragg-Brentano geometry (CuK<sub>α</sub> radiation).

Qualitative variable slit data were collected over  $2\theta$  angles of  $2^\circ$ - $40^\circ$ , using a step size of 0.02 and a run time of 1s/step. TEM samples were cut using a diamond knife and RMC MTXL ultramicrotome. The ultrathin sections were then placed on 400 mesh copper grids and photographed using a JEOL 100cx-II Transmission Electron Microscope operating at 80kV. UV transmission spectra were obtained using a Varian Cary 5000 UV-VIS-NIR spectrophotometer in the UV-Vis mode over 350 to 500 nm. Dynamic mechanical thermal analysis (DMTA) was performed using a Rheometric Scientific 3E apparatus in the rectangular tension/compression geometry.  $T_g$  is obtained from the maximum peak in the tan delta curves and crosslink densities are calculated from the  $E'$  value in the linear portion at least 50 °C greater than the  $T_g$ . Crosslink density can be calculated from the following equation:<sup>13</sup>

$$E = 3\nu_e RT \quad (1)$$

where  $\nu_e$  is the crosslink density. Sample sizes for test were  $(10 \times 5 \times (0.05 \text{ to } 0.09)) \text{ mm}^3$ . The analysis was carried out from 0 to 200 °C at a frequency of 10 rad/s and ramp rate of 5 °C/min. Hardness tests were performed utilizing a BYK Gardener pendulum hardness tester in the König mode in seconds. Samples for hardness testing were cured on an aluminum panel.

**Preparation of nanocomposite polymer films.** Polymer film formulations utilized in this study were 50:50 mixture of CN929:SR454, 50:50 mixture of CN121:SR454, and a 25:25:50 mixture of CN2251:CN2274:SR454. The clay loadings in these systems were 1, 3, and 5 wt%. Initiator Darocur 1173 (4 wt%) was added and mixture, stirred, then sonicated for 8 h. Films were cast onto glass, aluminum, and polysulfone panels using a #1 Gardco casting bar with a gap of 4 mil.

## Results and discussion

**Structure of the Nanoreinforced films.** Examination of the clay-polymer film structure can be done by x-ray diffraction (XRD) and transmission electron microscopy (TEM). In the case of XRD it is the shift in the  $d_{001}$  peak for the clay that is observed and a shift to lower 2-theta angles indicates intercalation while an absence of a peak suggests exfoliation. But one should be cautioned as to relying on this method as the sole method for identifying structure as an absence of a peak could be due to geometry effects. Therefore, it is widely accepted that to confirm the structure of a nanocomposite one must do TEM. **Figure 1** shows the TEM obtained for an urethane acrylate formulation and epoxy acrylate formulation containing 3 wt. % clay. From this it can be observed that intercalated structures are formed. There appears to be better dispersion in the case of the urethane acrylate than for the epoxy acrylate.

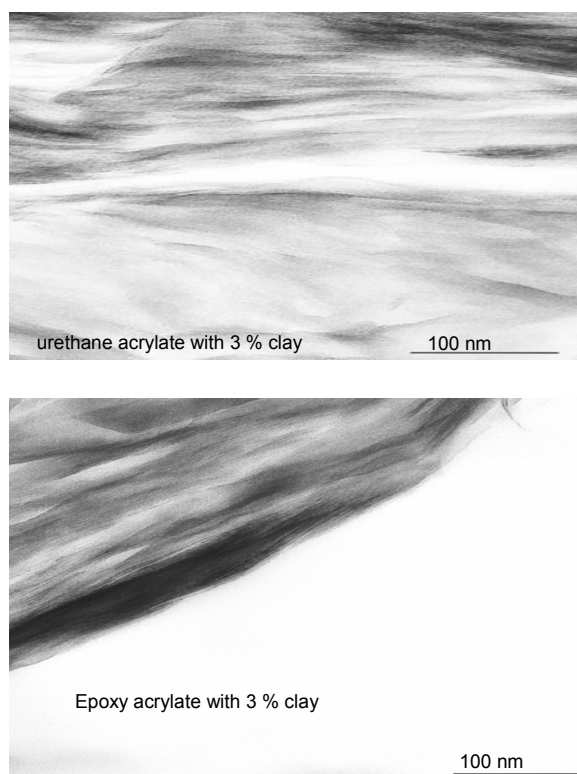


**Figure 1.** TEM of urethane acrylate (top) and epoxy acrylate (bottom) containing 3 wt. % clay.

**Optical clarity of films.** Optical clarity of the films can be assessed by UV-Visible spectra are shown in **Figure 2** for the epoxy acrylate with 3 wt. % clay and for the polyester acrylate with 3 wt. % clay. It should be noted that for the urethane acrylate films UV-visible behavior is similar to that of the epoxy acrylate. The epoxy acrylate films are only slightly affected by the presence of the clay, while the polyester acrylate shows a more pronounced effect due to the presence of the clay. That is the clay containing polyester acrylate formulations exhibit a lower optical transparency than either the clay containing urethane or epoxy acrylate formulation. The lower optical clarity could be due to the strong scattering of the montmorillonite clay which would result in the lower transparency of the UV-visible light.<sup>14, 15</sup>

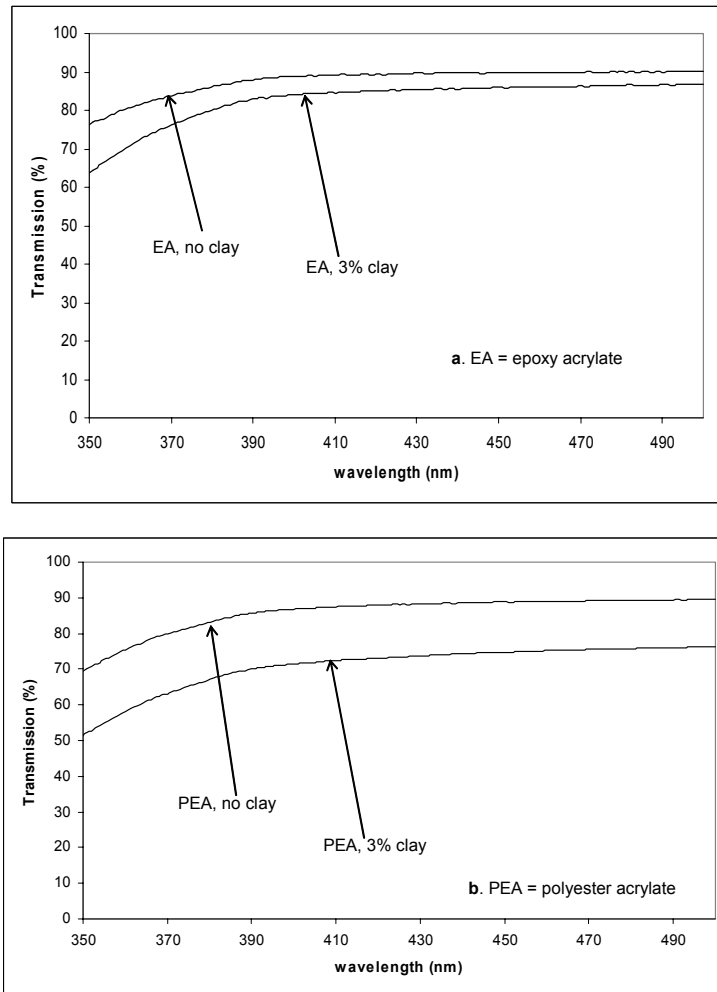


**Figure 2.** UV-visible spectra of epoxy acrylate (top) and polyester acrylate (bottom) with no clay and 3 wt. % clay.

**Cure time.** Cure is the crosslinking of a polymer to produce a three-dimensional network that is tack free. **Figure 3** shows the cure times obtained for the urethane acrylate, polyester acrylate, and epoxy acrylate formulations. It can be seen that as clay is added into the urethane acrylate formulations a decrease in cure time is observed, while for the epoxy acrylate there is no affect on cure time until the 5 wt. % loading at which point the cure time increases. In the case of the polyester acrylate, at the 1 wt. % loading an initial increase in cure time is observed but a decrease is noted at higher loadings.

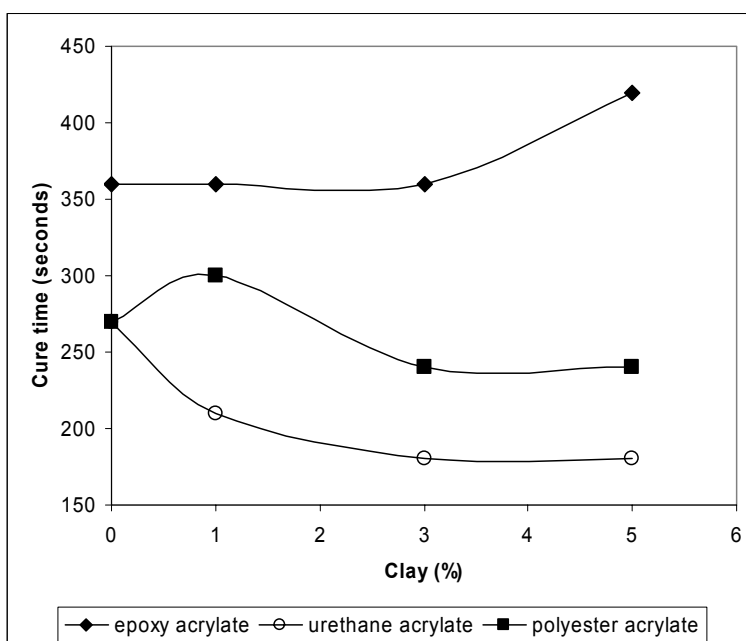


**Figure 4.** Cure times for the different acrylate formulations.

## Film Properties

Properties can be examined for the UV cured acrylate-clay films. Using DMTA the glass transition temperature ( $T_g$ ), crosslink density (XLD), and storage modulus ( $E'$ ) below and above  $T_g$  can be determined. **Figure 5** shows the effect of clay on  $T_g$  using DMTA. Urethane acrylate formulations containing clay appear to have no effect on glass transition temperatures while for the epoxy acrylate formulations at low loadings of clay the  $T_g$  appears to decrease and then increase at the 5 wt. % loading. For the polyester acrylate an increase in  $T_g$  occurs as the amount of clay is increased. In **Figure 6** an examination of XLD is shown for the various formulations. In this particular case the clay appears to enhance the effective crosslink density relative to the unmodified urethane acrylate. Epoxy acrylate formulations show a very small increase in XLD at the 3 and 5 wt. % loadings of clay, while for the polyester acrylates there appears to be a negligible affect on XLD due to the presence of the clay. It should also be noted that the polyester acrylate formulations have significantly higher XLDs relative to the urethane acrylate and epoxy acrylate formulations. **Table 3** give  $E'$  values above and below  $T_g$  for the various formulations. From this it can be observed that the urethane acrylate give a higher  $E'$  value below (20 to 40% increase) and above (15 to 20 % increase)  $T_g$ . The epoxy acrylate and polyester formulations show an mixture of  $E'$  values below  $T_g$ .  $E'$  values above  $T_g$  for the polyester acrylate exhibits very little change while for the epoxy acrylates an increase in  $E'$  above  $T_g$  is observed.

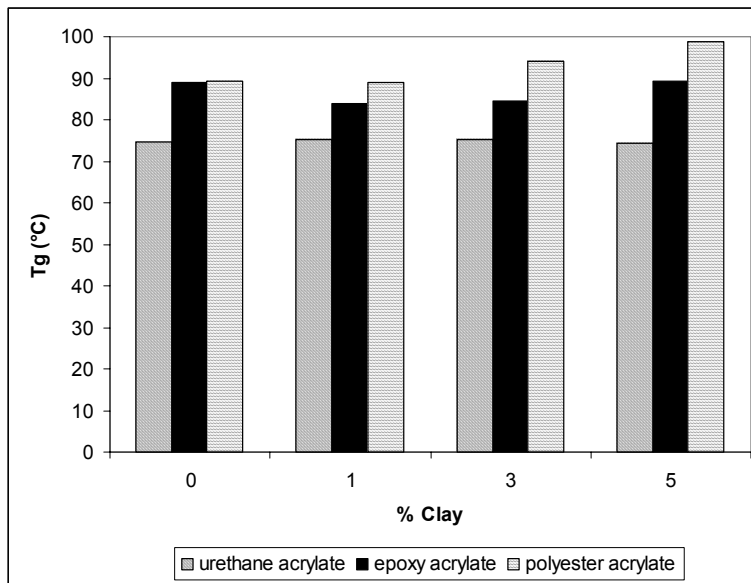


**Figure 5.** Glass transition temperatures by DMTA.

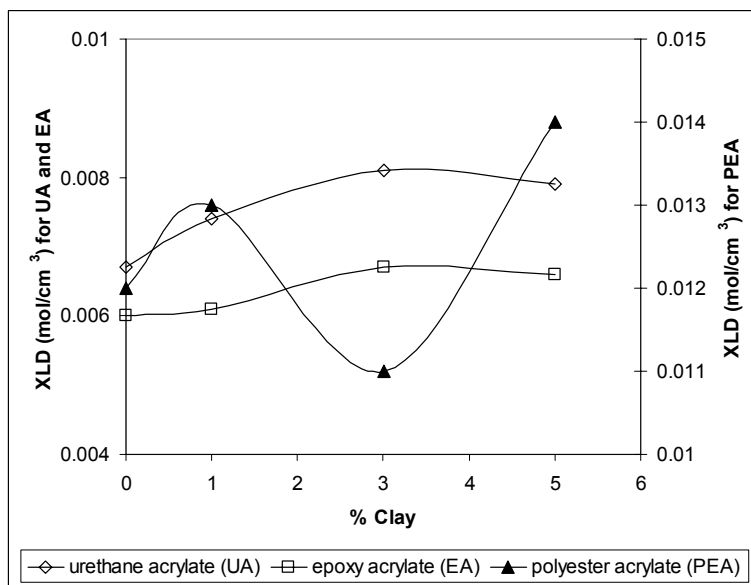


**Figure 6.** Crosslink densities (XLD) for acrylate formulations.

**Table 3.** E' values below and above T<sub>g</sub> for various acrylate formulations.

Sample	Clay (%)	E' @ 40 °C (GPa)	E' @ 175 °C (GPa)
Urethane acrylate	0	1.06	0.070
	1	1.23	0.080
	3	1.18	0.087
	5	1.28	0.084
Epoxy acrylate	0	2.03	0.066
	1	1.89	0.068
	3	2.20	0.073
	5	1.82	0.073
Polyester acrylate	0	1.08	0.13
	1	1.18	0.13
	3	0.96	0.12
	5	1.20	0.14

Hardness can be examined by the König pendulum hardness test, **Figure 7**. In this test a pendulum swings back and forth and the time required to dampen the movement from a high (6°) to low (3°) angle is recorded. For the urethane acrylate formulations a decrease in the König pendulum hardness is observed, while for the polyester acrylate formulations there is no effect until the 5 wt. % loading is reached and a slight decrease in hardness is seen. Epoxy acrylate formulations show an increase in the hardness as the amount of clay is increased.

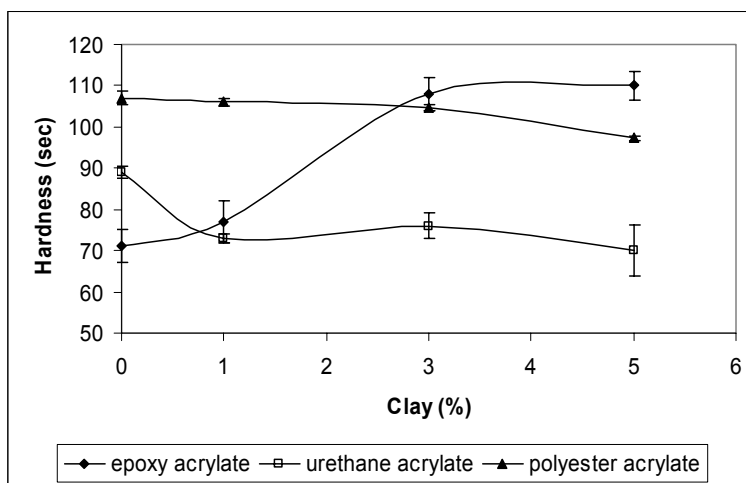


**Figure 7.** König pendulum hardness values for various acrylate formulations with clay.

## Conclusions

Structure-property relationships of several UV curable acrylate-clay formulations have been studied. Based on TEM it can be seen that we have prepared an intercalated structure. Optical clarity of the urethane and epoxy acrylate formulations is quite high even with the presence of the clay; only a change of 3 to 4 % transmittance is observed when clay is present relative to when there is no clay present. Polyester acrylates show a lower optical clarity in the presence of the clay, a decrease of ~ 15 % transmittance. It can be seen that the effect of the clay on film properties is dependent upon the acrylate used. Hardness increases upon incorporation of clay into the formulation for the epoxy acrylate while the urethane acrylate exhibits a decrease and the polyester acrylate shows no effect on hardness upon addition of clay.  $T_g$  (DMTA) increases for the polyester acrylates and at high loadings of clay in the epoxy acrylate formulations but in the case of the urethane acrylate formulations there is no effect on  $T_g$ .

## Acknowledgments

The authors thank the Center for Nanoscale Science and Engineering (CNSE) and the Defense Microelectronics Activity (DMEA), contract number DMEA-90-02-C-0224, for support of this research. One of us (SCW) acknowledges the support of NSF SGER Grant # CMS 0335390 on nanocomposites administered by the Mechanics and Materials Program.

## References

- (1) Jackson, P., **2002** *Paint and Resin Times*, 1, 26.
- (2) Fouassier, J. P., *Photoinitiation, Photopolymerization, and Photocuring Fundamentals and Applications*, Hanser Publishers, New York, **1995**, p. 246.
- (3) Koleske, J. V. Ed. ASTM International, Pennsylvania, **2002**, p. 79.
- (4) Schwalm, R., **1998** *Polym. Paint Coat J.*, 18.
- (5) Schwalm, R., Haubling, L., Reich, W., Beck, E., Enenkel, P., Menzel, K., **1997** *Prog. Org. Coat.*, 32, 191.
- (6) Schwalm, R., Haubling, L., Reich, W., Beck, E., Enenkel, P., Menzel, K., Keil, E., **1997** *Modern Paint and Coat*, 87, 42.

- (7) Alexandre, M., Dubois P, **2000** Mater Sci. Eng., *R28*, 1-63.
- (8) Ogawa, M., Kuroda K, **1997** Bull. Chem. Soc. Jpn., *70*, 2593-2618.
- (9) Wang, W. J., Chin W-K, **2002** J. Polym. Sci. Part B: Polym. Physics, *40*, 1690-1703.
- (10) Tortora, M., Gorrasi G, Vittoria V, Galli G, Ritrovati S, Chiellini E, **2002** Polym., *43*, 6147-6157.
- (11) Wu, J., Lerner, M. M., **1993** Chem. Mater., *5*, 835-838.
- (12) Carrado, K. A. in *Vol.* (Ed. G Shonaik, Advani SG), CRC Press, **2003**, pp. 349-396.
- (13) Wicks, Z. W. Jr, Jones FN, Pappas SP, *Organic Coatings*, John Wiley & Sons, New York, **1999**, p. 71.
- (14) Yeh, J.-M., Liou, S.-J., Lin, C.-Y., Cheng, C.-Y., Chang, Y.-W., **2002** Chem. Mater., *14*, 154.
- (15) Yu, Y.-H., Lin, C.-Y., Yeh, J.-M., Lin, W.-H., **2003** Polym., *44*, 3553.